MANE-6960
Vignesh Ramakrishnan
Due: Friday September 27, 2024

Assignment 1

The Poisson type PDE is defined on the square domain $\Omega \in [0,1]^2$ with Dirichlet boundary conditions:

$$\begin{aligned} -\nabla \cdot (\gamma \nabla u) &= f, && \forall (x,y) \in \Omega, \\ u(x,y) &= u_\Gamma(x,y), && \forall (x,y) \in \Gamma. \end{aligned} \tag{1}$$

The solution and diffusion coefficient are, respectively,

$$u\,(x,y) = e^y \sin \frac{\pi\,(e^x - 1)}{e-1}, \text{ and, } \gamma(x) = \frac{\pi e^x}{e-1}. \tag{2}$$

Using the method of manufactured solutions, the load is determined to be,

$$f(x,y) = -\left\{ u(x,y)\gamma\left(1-\gamma^2\right) + 2\gamma \frac{\partial u(x,y)}{\partial x} \right\}. \tag{3}$$

1. Deriving the adjoint formulation for the PDE and the objective

$$\begin{aligned} (\psi, \mathcal{L}u)_\Omega &= -\int_\Omega \psi\,(\gamma u_{,i})_{,i}\; d\Omega \\ &= -\int_\Omega (\psi\gamma u_{,i})_{,i}\, d\Omega + \int_\Omega \gamma\psi_{,i} u_{,i} d\Omega \\ &= -\int_\Gamma \psi\,(\gamma u_{,i} n_i)\, d\Gamma + \int_\Omega (\gamma\psi_{,i} u)_{,i}\, d\Omega + \int_\Omega u\,(-\gamma\psi_{,i})_{,i}\, d\Omega \\ &= \int_\Gamma \psi\,(-\gamma u_{,i} n_i)\, d\Gamma - \int_\Gamma u\,(-\gamma\psi_{,i} n_i)\, d\Gamma + (u, \mathcal{L}^*\psi)_\Omega \end{aligned}$$

From the compatiblity condition,

$$(\psi, \mathcal{L}u)_\Omega - (u, \mathcal{L}^*\psi)_\Omega = (\mathcal{C}u, \mathcal{B}^*\psi)_\Gamma - (\mathcal{B}u, \mathcal{C}^*\psi)_\Gamma\,, \tag{4}$$

$$\begin{aligned} \mathcal{L} &\equiv -\nabla\cdot(\gamma\nabla)\,, & \mathcal{L}^* &\equiv -\nabla\cdot(\gamma\nabla)\,, \\ \mathcal{C} &\equiv -\hat{n}\cdot(\gamma\nabla)\,, & \mathcal{C}^* &\equiv -\hat{n}\cdot(\gamma\nabla) \\ \mathcal{B} &\equiv 1, & \mathcal{B}^* &\equiv 1. \end{aligned}$$

$$\mathcal{J}\,(u) = \int_{\Gamma_1} \beta\gamma\,(\hat{n}\cdot\nabla u)\, d\Gamma_1 \tag{5}$$

$$\begin{aligned} \mathcal{J}\,(u) &= (g, u)_\Omega + (c, \mathcal{C}u)_\Gamma && (6) \\ &= -\underbrace{(u, \mathcal{L}^*\psi - g)_\Omega}_{I} - \underbrace{(\mathcal{C}u, \mathcal{B}^*\psi - c)_{\Gamma_1}}_{II} + (f, \psi)_\Omega + (b, \mathcal{C}^*\psi)_\Gamma && (7) \end{aligned}$$

Comparing Equation (5) to Equation (7), $g = 0, c = \beta$. Setting I, II to 0, the adjoint formulation of the PDE is stated as,

$$\mathcal{L}^*\psi = 0, \; \forall x \in \Omega, \tag{8}$$
$$\mathcal{B}^*\psi = \beta, \; \forall x \in \Gamma_1, \tag{9}$$
$$\mathcal{B}^*\psi = 0.0, \; \forall x \in \Gamma \backslash \Gamma_1. \tag{10}$$

2. Implementing an adjoint consistent discretization for Equations (1) and (2).
The weak form of the primal PDE is,

$$-\int_\Gamma v\left(\gamma u_{,i} n_i\right) d\Gamma + \int_\Omega v_{,i}\gamma u_{,i} d\Omega = \int_\Omega v f d\Omega.$$

In order to achieve adjoint consistency, the Dirichlet boundary conditions have to be weakly imposed. The following terms,

$$-\int_\Gamma \left(\gamma v_{,i} n_i\right)\left(u - u_\Gamma\right) d\Gamma + \frac{\kappa}{h}\int_\Gamma (\gamma v)\left(u - u_\Gamma\right) d\Gamma,$$

are added to the weak-form to maintain coercivity (positive definiteness) and to weakly impose Dirichlet boundary conditions.

$$\underbrace{\int_\Omega v_{,i}\gamma u_{,i} d\Omega}_{A} + \underbrace{\sigma\int_\Gamma \left(\gamma v_{,i} n_i\right) u \, d\Gamma - \int_\Gamma v\left(\gamma u_{,i} n_i\right) d\Gamma + \frac{\kappa}{h}\int_\Gamma \gamma u v \, d\Gamma}_{B} =$$
$$\underbrace{\int_\Omega v f d\Omega}_{C} + \underbrace{\sigma\int_\Gamma \left(\gamma v_{,i} n_i\right) u_\Gamma d\Gamma + \frac{\kappa}{h}\int_\Gamma u_\Gamma \gamma v \, d\Gamma}_{D}, \tag{11}$$

where $\sigma = -1$, and $\kappa = (p+1)^2$ with p being the order of the polynomial function space used in the discretization of both the test function $v \in \mathcal{V}$ and the trial function $u \in \mathcal{U}$. The primal problem was discretized using H^1 continuous quadratic ($p = 2$) Finite Elements and was solved using PyMFEM. The following integrators in PyMFEM,

$A \equiv$ DiffusionIntegrator,	$B \equiv$ DGDiffusionIntegrator,
$C \equiv$ DomainLFIntegrator,	$D \equiv$ DGDirichletLFIntegrator,

were used to generate the bilinear and linear forms respectively. The integrators B, D were only applied to the Dirichlet Boundary Faces. A mesh-convergence study revealed errors with higher than a second-order rate of convergence ≈ 2.92, in the L^2 norm as shown in Fig.1.

3. Solving the discrete adjoint problem
In order to account for the weak imposition of Dirichlet Boundary conditions, we need to add a penalty term to the functional $\mathcal{J}(u)$. This objective functional in the continuous form is modified to,

$$\mathcal{J}(u) = \int_{\Gamma_1} \beta\left(\left(\gamma\hat{n}\cdot\nabla u\right) + \frac{\kappa}{h}\gamma\left(u - u_{\Gamma_1}\right)\right) d\Gamma_1.$$

This integral is discretized as,

$$\mathcal{J}(u) = \left(u, \left(\beta, \gamma\hat{n}\cdot\nabla v + \frac{\kappa}{h}\gamma v\right)\right) - \left(1, \left(\beta u_{\Gamma_1}, \gamma v\right)\right).$$

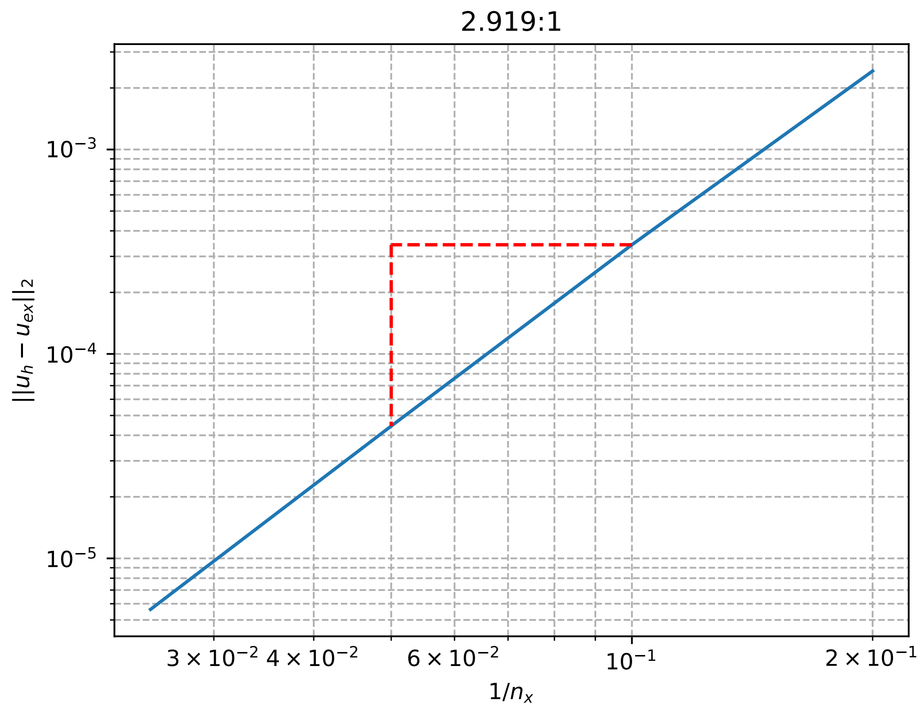

Figure 1: Rate of convergence of the L^2 solution error versus the mesh size n_x

This is achieved in PyMFEM by finding the inner product of the state variables u_h with the linear form g_h given by the numerical integration of the functional,

$$-\sigma \int_{\Gamma_1} \beta\gamma\hat{n}\cdot\nabla v \; d\Gamma_1 + \frac{\kappa}{h}\int_{\Gamma_1} \gamma v \; d\Gamma_1,$$

and adding it to the correction term given by the inner product of a vector of ones with the discretized numerical integration of the functional,

$$-\frac{\kappa}{h}\int_{\Gamma_1} \gamma u_{\Gamma_1} v \; d\Gamma_1.$$

Therefore, the discrete functional is given by,

$$J_h\left(u_h\right) = g_h^T u_h + \mathbf{1}^T c_h.$$

The Lagrangian of the discretized version of the primal problem is,

$$Lg\left(u\right) = g_h^T u_h + +\mathbf{1}^T c_h + \psi_h^T\left(L_h u_h - f_h\right).$$

The discrete adjoint variables are calculated by setting,

$$\frac{\partial Lg}{\partial u_h} = L_h^T\psi_h + g_h = 0.$$

(a) Solving for the choice $\beta\left(x\right) = 1$
The contours of the discrete adjoint variables and the mesh convergence study of the error in functional computation is shown in Fig.2. This is not super-convergent because the adjoint variables are discontinuous at the boundaries $x = 0$ and $x = 1$ where $\beta(0) = \beta(1) = 1$ when technically it should have been 0.

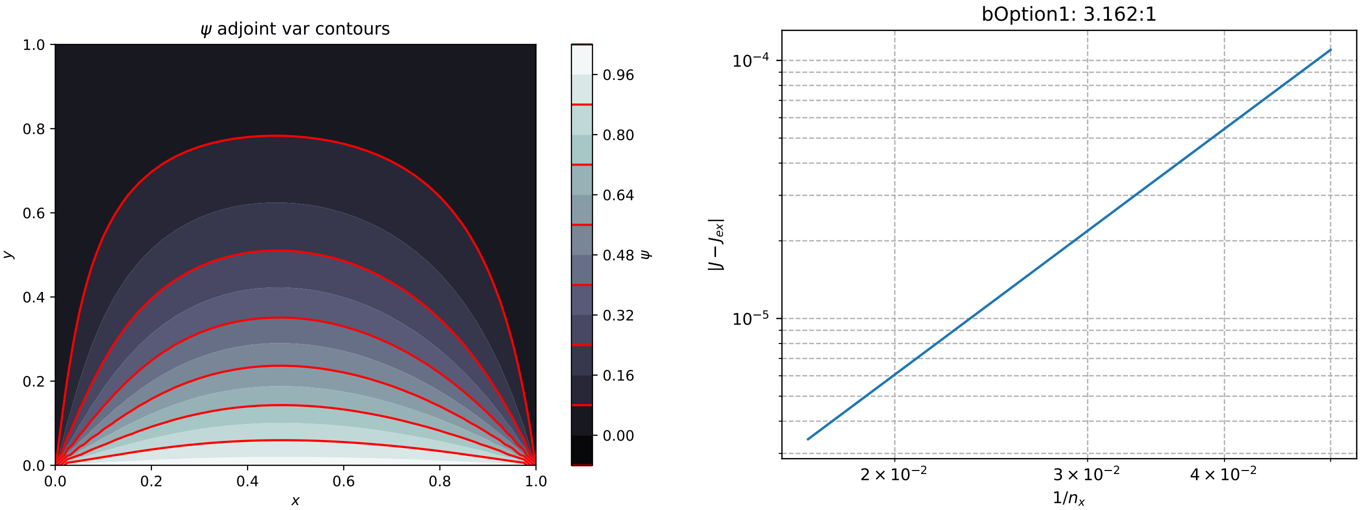

Figure 2: (a) Countours of the adjoint variables, (b) mesh convergence study of the functional error $|J - J_{\text{ex}}|$ versus mesh size $1/n_x$

(b) Solving for the choice $\beta\left(x\right) = \frac{\pi^2 (e^x - 1)(e - e^x)}{(e-1)^2}$
The contours of the discrete adjoint variables and the mesh convergence study of the error in functional computation is shown in Fig.3. This is super-convergent because the boundary

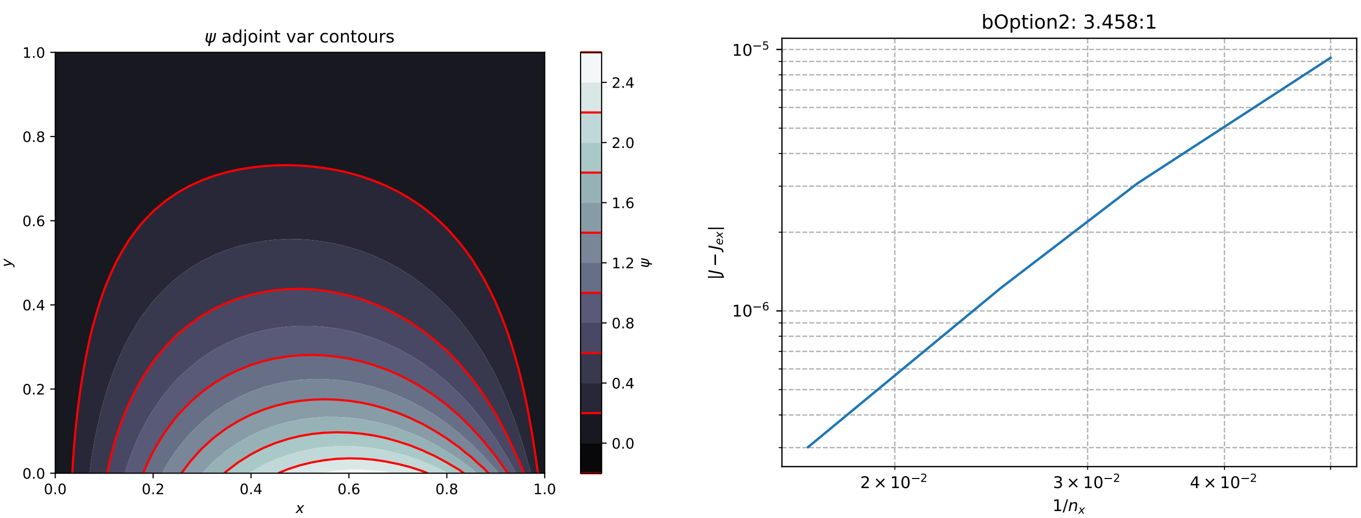

Figure 3: (a) Countours of the adjoint variables, (b) mesh convergence study of the functional error $|J - J_{\text{ex}}|$ versus mesh size $1/n_x$

conditions are not discontinuous at $x = 0$ and at $x = 1$ since $\beta(0) = \beta(1) = 0$.